POWDER STATE CHARACTERIZATION OF ZnO/C and NiO/C COMPOSITE NANOPOWDERS SYNTHESIZED VIA SPRAY DRYING SUBSEQUENT THERMAL DECOMPOSITION

M.Sc. Duman Ş., Assoc. Prof. Dr. Özkal B.
Istanbul Technical University, Metallurgical and Materials Engineering Department, PML Laboratories,
34469, Maslak, Istanbul, Turkey
dumanseyma@gmail.com, ozkal@itu.edu.tr

Abstract: *In this study, ZnO/C and NiO/C composite nanopowders were synthesized via spray drying subsequent thermal decomposition. Citric acid was used as a carbon source in spray drying slurry containing zinc acetate or nickel acetate powders. Spray drying conditions like inlet temperature, feed rate and drying air flow rate were adjusted 200 ^oC, 3 ml/min. and 800 ml/min, respectively. The composites were composed of amorphous carbon and nanopowders ZnO and NiO by thermally decomposing at 300 oC for 4 h in Ar atmosphere of spray drying powders. The synthesized nanopowders of powder state characterization were performed. SEM examinations demonstrated that the morphologies of ZnO/C composite nanopowders have spherical structures with dents and wrinkles on their surfaces are promoted with the addition of carbon. It was observed from XRD results that synthesized powders had hexagonal wurtzite structure for ZnO/C nanopowders and face centered cubic structure for NiO/C nanopowders. The existence of carbon into the composite nanopowders was detected by EDS and Raman microanalyses. The carbon doping was increased surface areas and decreased crystallite sizes.*

Keywords: ZnO/C, NiO/C, SPRAY DRYING, THERMAL DECOMPOSITION, RAMAN SPECTROSCOPY

1. Introduction

ZnO and NiO are direct large band gap (3.37 eV and 3.6 eV, respectively) semiconductors, which have been commonly investigated due to theirs low cost, nontoxic, nature friendly, high photosensitivity and high stability properties [1-3]. Carbon (C) can be used as a good organic matter and ZnO and NiO nanopowders with doping C are found to display high chemical stability, high mechanical strength, superior photocatalytic properties, remarkable optical and electronical properties compared to pure ZnO and NiO [4, 5]. Meanwhile, the carbon doped materials with large specific surface area can be preferred for many potential applications, including lithium-ion batteries [1], fuel cells [6], supercapacitors [7] and photocatalyst [8].

ZnO and NiO nanoparticles have been synthesized from aqueous solutions of different zinc and nickel salts (acetate, nitrate or sulfate), respectively. The widely used carbon sources are citric acid, glucose, sucrose, polyvinyl alcohol [9-12]. ZnO/C and NiO/C systems have been successfully synthesized a few methods such as thermal decomposition, pyrolysis, sol-gel and chemical vapour deposition [10-12]. The homogeneous and uniform distribution represent a considerable challenge to obtain well-dispersed ZnO/C and NiO/C composite nanopowders. Thermal decomposition method could remain incapable of synthesizing homogeneously ZnO/C and NiO/C composite nanopowders. As a preliminary process, spray drying, which is transformed from feed slurry to a dry granule by spraying into hot medium, can be used 13, 14]. Spray drying and subsequent thermal decomposition combination was successfully applied to prepare anode material for lithium ion batteries [13, 15, 16]. There are not sufficient studies in the literature on synthesizing of ZnO/C and NiO/C composite nanopowders by spray drying and subsequent thermal decomposition in argon (Ar) atmosphere.

In the present work, we investigated the synthesis of ZnO/C and NiO/C composite nanopowders by spray drying and subsequent thermal decomposition processes. The characterization of these composite powders was conducted using scanning electron microscopy (SEM), energy dispersive spectroscopy (EDS), nano-particle size distribution (Nano-PSD), specific surface area measurement (BET), X-ray diffractometer (XRD), raman spectroscopy, apparent and true density measurements.

2. Experimental Procedure

Zinc acetate dehydrate ($Zn(CH_3COO)_2 \cdot 2H_2O$ Alfa AesarTM), nickel acetate dehydrate ($Ni(CH_3COO)_2 \cdot 4H_2O$ Alfa AesarTM) and citric acid ($C_6H_8O_7$, Sigma AldrichTM) all in powder form were selected as starting materials. Aqueous solutions of 0.5 M zinc acetate (hereafter $Zn(Ac)_2$) and 0.5 M nickel acetate (hereafter $Ni(Ac)_2$) were separately prepared by dissolving it in distilled water (50 ml). For the preparation of samples having carbon, 0.3 M citric acid (hereafter CA) was added into the zinc acetate solution and stirred to obtain homogeneous and stable solutions at 80 ^oC for 1 hour. Both prepared solutions were spray dried prior to thermal decomposition using a laboratory-scale Büchi brand Mini Spray Dryer B-290. Spray drying conditions like inlet temperature, outlet temperature, feed rate and drying air flow rate were adjusted 200 ^oC, 110 ^oC, 3 ml/min. and 800 ml/min, respectively. The composites were composed of amorphous carbon and ZnO or NiO nanopowders by thermally decomposing at 300 °C in Ar atmosphere of spray drying powders. Thermal decomposition experiments of spray dried granules were realized in a muffle type furnace with a heating rate of 2 °C/min and 4 h dwell time at peak temperature and then the samples were furnace cooled. A supplementary flow chart is given in Figure 1 to summary the experimental details.

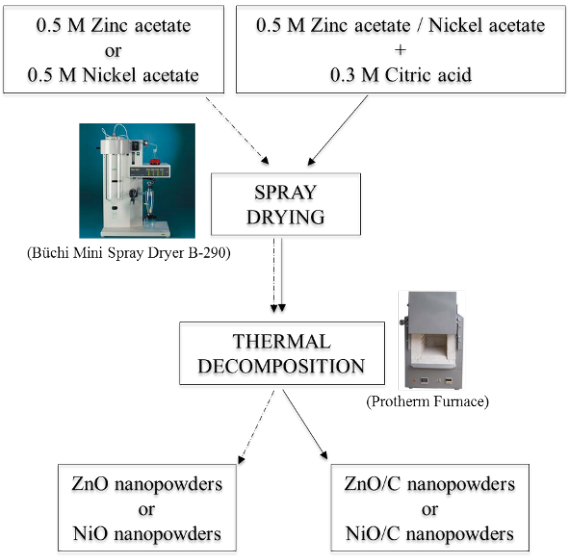

Figure 1. *The flow chart showing the applied procedure for prepared samples.*

A variety of characterization techniques were applied adter synthesis. In order to examine particle morphology, SEM observations and EDS microanalyses were carried out for all synthesized nanopowders using Quanta^{TM} FEG 250. Particle size measurements of the powders were conducted using Microtrac^{TM} Stabino Particle Size Distribution. The specific surface area of the synthesized nanopowders prepared in this study was measured

using the Brunauer–Emmett–Teller (BET) method via Quantachrome™ Autosorb-1 MP device. For this purpose, all samples were outgassed for at least 12 h at 80 °C prior to the adsorption measurements. XRD analyses were performed using Bruker D8 Advance in 2θ mode, Cu anode at 40 kV and 35 mA. Measurements were scanned from 20° to 80° with a step size of 2°/min on the 2θ. Raman spectroscopy was recorded on a JY HR-800 (Jobin Yvon Horiba™). The apparent and true densities were measured with Arnold density measurement kit and helium pycnometer (Micromeritics™, Accupyc 1330), respectively.

3. Results and Discussion

In our previous study [13], we successfully synthesized nanosized particles using spray drying and subsequent thermal decomposition processes in consequence of decomposition reaction of zinc acetate into ZnO. In this study, similar processes were used and ZnO/C and NiO/C were synthesized by utilizing citric acid as a carbon source. The SEM images of the synthesized ZnO and ZnO/C nanopowders are given in Figure 2. While ZnO nanoparticles (Figure 2a) had rod-like structures, doping with carbon (Figure 2b) led to mostly spherical structures with wrinkles on their surfaces. The chemical composition of the ZnO/C composite nanopowders was determined by EDS, as displayed in Fig. 2c, in order to showing the presence of the Zn, O and C elements. EDS analysis of the ZnO/C composite nanopowders confirmed the existence of carbon and the content of carbon in the composite can be calculated to be ~17 wt%.

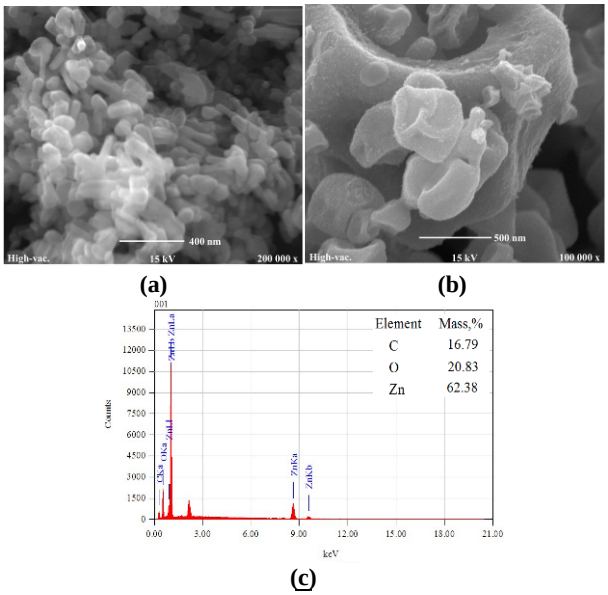

Figure 2. *SEM micrographs and the synthesized nanopowders: a) ZnO, b) ZnO/C and c) EDS microanalyses of ZnO/C.*

As seen in the Figure 3, NiO nanoparticles formed rod structures, whereas NiO/C composite nanoparticles have spherical structures with small dents and wrinkles on their surfaces. Dents and wrinkles on the surfaces were formed using citric acid during spray drying. It was previously reported in the article by Özgüven et. al [17] that high solvent evaporation rates may lead to collapse of particles. It is very clear that the addition of carbon plays a key role for change of morphology. EDS miroanalysis of the NiO/C composite powders is shown in Figure 3c, which demonstrates the existence of elements of Ni, O and C. The peaks of NiO were observed, indicating that the carbon in the composite powders is amorphous. EDS analysis of the NiO/C composite nanopowders confirmed the existence of carbon, the content of which in the composite is about 7.5 wt.%.

Particle size and the surface area measurements of the synthesized nanopowders are given in Table 1. While the particle size measurements for ZnO and ZnO/C nanopowders were 306 nm and 235 nm respectively, in order of similar values for NiO and NiO/C nanopowders were 414 nm and 330 nm. Both in ZnO and NiO systems, the decrease in particle size with doping carbon were observed. It was found that the BET surface area was 18.50 and 25.91 m^2/g for the ZnO nanopowders and the ZnO/C composite nanopowders, respectively. The BET surface area was found to be 23.12 and 136.0 m^2/g for the NiO nanopowders and the NiO/C composite nanopowders, respectively. On the other hand, an increase in BET values was observed due to the effect of carbon doping.

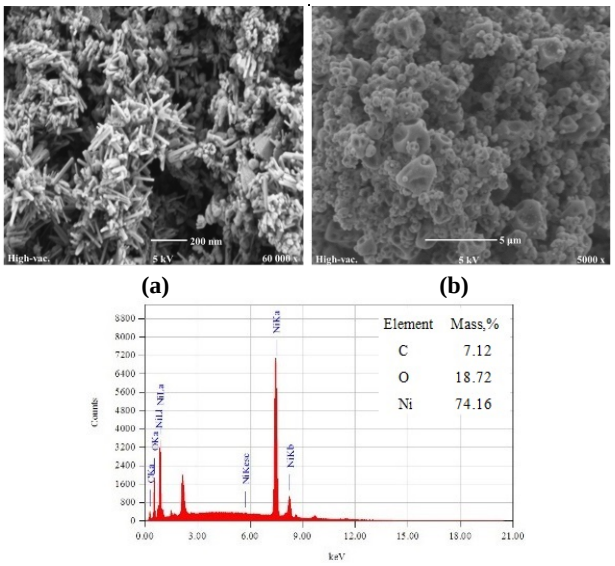

Figure 3. *SEM micrographs and the synthesized nanopowders: a) NiO, b) NiO/C and c) EDS microanalyses of NiO/C.*

Theoretical density of ZnO and NiO are 5.61 g/cm^3 and 6.67 g/cm^3, respectively. Apparent and true densities of the synthesized nanopowders are given in Table 1. When the apparent densities for ZnO and ZnO/C nanopowders were 0.42 g/cm^3 and 0.79 g/cm^3 respectively, in order of true density values for ZnO and ZnO/C nanopowders were 5.58 g/cm^3 and 5.22 g/cm^3. Also for NiO and NiO/C nanopowders, the apparent densities were 0.65 g/cm^3 and 0.98 g/cm^3 and true densities were 5.58 g/cm^3 and 5.22 g/cm^3, respectively. Both in ZnO and NiO systems, the decrease in true densities with doping carbon were observed. ZnO and NiO nanopowders exhibited poor flow and packing characteristics due to formation rod-like and irregular structures. The synthesized composite nanopowders doping with carbon led to mostly spherical structures and certainly improved the packing behaviors.

Table 1. *Physical properties of the synthesized nanopowders.*

Sample	*Particle Size (nm)*	*Specific surface area (m^2/g)*	*Apparent Density (g/cm^3)*	*True Density (g/cm^3)*
ZnO	306	18.50	0.42	5.58
ZnO/C	235	25.91	0.79	5.22
NiO	414	23.12	0.65	6.61
NiO/C	330	136.0	0.98	6.15

Fig. 4a presents the XRD patterns of ZnO and ZnO/C nanopowders by thermal decomposition of the spray dried powders. The intense peaks of ZnO having good crystalline qualities were confirmed. The peaks originated from (100), (002), (101), (102), (110), (103), (200) and (112) may be indexed. Characteristic ZnO peaks which is good agreement with the JCPDS card no. 70-8070 (wurtzite hexagonal phase) was detected as major phase. [13]. The position of the peaks was slightly shifted toward higher angles due to carbon doping. Moreover, the peaks intensity of ZnO/C composite nanopowders decreased compared to ZnO nanopowders.

Fig. 4b shows the XRD patterns of the NiO and NiO/C nanopowders by thermal decomposition of the spray dried powders.

XRD patterns showed five diffraction peaks at 2θ of 37.12°, 43.16°, 62.77°, 75.30° and 79.29°, which are referred to (111), (200), (220), (311), (222) planes of face centered cubic NiO phase [1, 2]. No characteristic peaks of carbon or any impurity peaks were observed via XRD, indicating that the synthesized nanopowders were composed of a single ZnO or NiO phase.

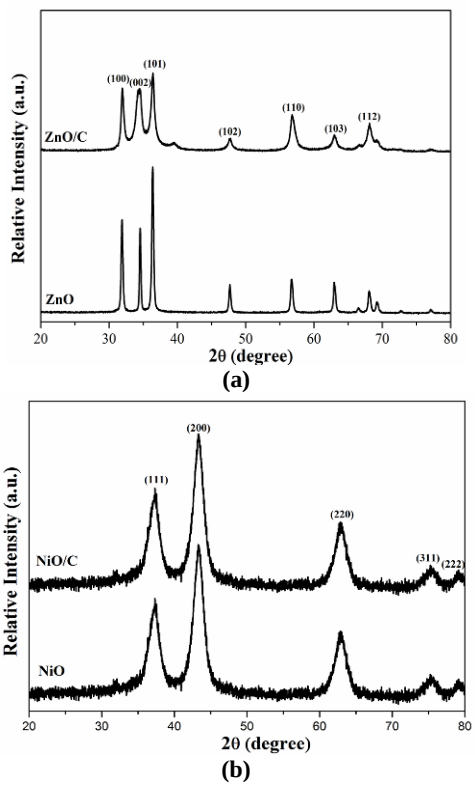

Figure 4. *XRD patterns of the synthesized nanopowders by thermal decomposition of the spray dried powders: a) ZnO, b) ZnO/C, c)NiO and d) NiO/C.*

Table 2 *shows that the average crystallite sizes (D) were calculated by Debye-Scherrer's equation [5, 13] from the highest intense peaks (101) and (200) of ZnO and NiO, respectively:*

$$D = \frac{k\lambda}{\beta \cos\theta} \quad (1)$$

where β is the corrected half-peak width of the experimental sample (FWHM), θ is Bragg angle, λ = is the X-ray wavelength (1.54˚A), and k is the shape factor of value 0.9. The crystallite size of the synthesized samples by thermal decomposition of the spray dried powders were estimated. As it can be seen from Table 2, the crystallite size decreased with carbon doping, as 2θ value increased. According to XRD parameters, the carbon doping was increased surface areas and decreased the crystallite sizes of ZnO and NiO nanopowders, which is quite similar to the findings of Bechambia et al. [5]. Besides, crystallite sizes decreased and strain rates increased as it was expected.

Table 2. *XRD parameters of the synthesized samples by thermal decomposition of the spray dried powders.*

Sample	*2θ*	*hkl*	*Crystallite size (nm)*	*Strain (%)*
ZnO	36.71	(101)	28.1	0,0014
ZnO/C	36.78	(101)	25.9	0,0007
NiO	43.50	(200)	89.2	0.0173
NiO/C	43.61	(200)	83.7	0.0092

Raman microanalysis is an important technique in the characterization of ZnO/C and NiO/C composite nanopowders. Raman spectrum of ZnO/C composite nanopowders is presented in Figure 5. Two broad peaks at about 1340 and 1590 cm^{-1} were obviously observed, which could be marked as the defect induced line (D) and the graphitic line (G) bands of carbon, respectively [18, 19]. The small peak at about 420 cm^{-1} may be referred to Zn–O stretching of ZnO [19]. This result indicates that the Sample 1 is ZnO/C composites. Some amount of carbon existed and incorporated into ZnO and NiO structures, as evidenced by EDS (Figure 2c and 3c) and Raman (Figure 5) microanalyses.

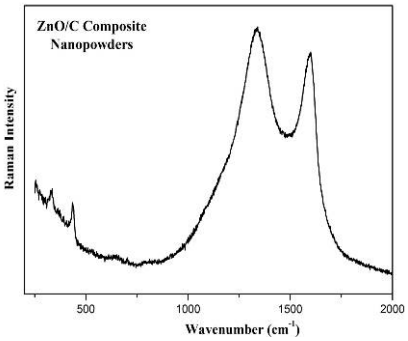

Figure 5. *Raman spectroscopy of the synthesized ZnO/C composite nanopowders.*

4. Conclusions

The effects of the citric acid addition on the morphology of the ZnO and NiO nanopowders synthesized via spray drying and subsequent thermal decomposition processes have been investigated in the present study. Based on the obtained results, following conclusions can be drawn:

1. Microstructural characterizations by SEM revealed that the synthesized ZnO and NiO nanopowders have rod-like structures and composite nanopowders, in which spherical structures with dents and wrinkles on their surfaces are promoted with the addition of carbon.
2. XRD patterns of the synthesized ZnO and ZnO/C nanopowders revealed the presence of a single wurtzite ZnO phase. The characteristic peaks of face centered cubic phase NiO was detected for the synthesized NiO and NiO/C nanopowders.
3. The carbon doping was increased surface areas and 2θ value, as the crystallite sizes and strain rates of ZnO and NiO systems decreased.
4. The existence of carbon into ZnO/C and NiO/C composite structures was evidenced by EDS and Raman microanalyses.

Acknowledgement

This work is supported by ITU-BAP 36459 project. Authors would like to thank Res.Asst. Sıddıka Mertdinç and MSc. Merve Küçük for their great contribution.

References

[1]. J. Zhang, S. Ni, J. Tang, X. Yang, L. Zhang, The preparation of NiO/C-Ni composite as binder free anode for lithium ion batteries, Mater. Lett. 176 (2016) 21–24.

[2]. Z. Cui, H. Yin, Q. Nie, Controllable preparation of hierarchically core-shell structure NiO/C microspheres for non-enzymatic glucose sensor, J. Alloys Compd. 632 (2015) 402–407.

[3]. R. Aladpoosh, M. Montazer, The role of cellulosic chains of cotton in biosynthesis of ZnO nanorods producing multifunctional properties: Mechanism, characterizations and features, Carbohydr. Polym. 126 (2015) 122–129.

[4]. Y. Xiao, W. He, C. Gao, M. Zheng, B. Lie, X. Liu, Y. Liu, Controllable synthesis of hexagonal ZnO-carbon core-shell microrods and the removal of ZnO to form

hexagonal carbon microtubes, Mater. Chem. Phys. 140 (2013) 350–356.

[5]. O. Bechambia, S. Sayadi, W. Najjar, Photocatalytic degradation of bisphenol A in the presence of C-doped ZnO: Effect of operational parameters and photodegradation mechanism, J. Ind. Eng. Chem. 32 (2015) 201–210.

[6]. A.L. Dicks, The role of carbon in fuel cells, J. Power Sources 156 (2006) 128–141.

[7]. A. Janes, H.S. Kurig, E. Lust, Characterization of activated nanoporous carbon for supercapacitor electrode materials, Carbon 45 (2007) 1226–1233.

[8]. T. Chena, S. Yua, X. Fanga, H. Huanga, L. Lia, X. Wange, Enhanced photocatalytic activity of C@ZnO core-shell nanostructures and its photoluminescence property, Applied Surface Science 389 (2016) 303–310.

[9]. H. Zhao, Lithium Titanate-Based Anode Materials, In Rechargeable Batteries; Zhang, Z., Zhang, S. S., Eds.; Green Energy and Technology; Springer International Publishing: New York, (2015) 157-187.

[10]. B. Özkal, W. Jiang, S. Kato, O. Yamamoto, Z. Nakagawa, Characterization of Carbon-Coated ZnO Composite Powders Produced by Polymer Pyrolysis Method, J. Ceram. Soc. Jpn. 113 (2005) 116-119.

[11]. B. Özkal, W. Jiang, O. Yamamoto, K. Fuda, Z. Nakagawa, Preparation and characterization of carbon-coated ZnO and CaO powders by pyrolysis of PVA, J. Mater. Sci. 42 (2007) 983-988.

[12]. A. Kołodziejczak-Radzimska, T. Jesionowski, Zinc Oxide-From Synthesis to Application: A Review, Materials **7** (2014) 2833-2881.

[13]. Ş. Duman and B. Ozkal, Effect of dopant and binder on the formation of ZnO powders during thermal decomposition of spray dried zinc acetate based granules, Optoelectron. Adv. Mater.-Rapid Commun. 18 (2016) 705-711.

[14]. G. Bertrand, P. Roy, C. Filiatre, C. Coddet, Spray dried ceramic powders:A quantitative correlation between slurry characteristics and shapes of the granules, Chem. Eng. Sci. 60 (2005) 95-102.

[15]. B. Lin, Z.Y. Wen, Z.H. Gu and S.H. Huang, Morphology and electrochemical performance of $Li[Ni_{1/3}Co_{1/3}Mn_{1/3}]O_2$ cathode material by a slurry spray drying method, J. Power Sources 175 (2008) 564-569.

[16]. I. Taniguchi, N. Fukuda and M. Konarova, Synthesis of spherical $LiMn_2O_4$ microparticles by a combination of spray pyrolysis and drying method, Powder Technol. 181 (2008) 228–236.

[17]. M. Özgüven, A. Karadağ, Ş. Duman, B. Özkal, B. Özçelik, Fortification of dark chocolate with spray dried black mulberry (Morus nigra) waste extract encapsulated in chitosan-coated liposomes and bioaccessability studies, Food Chemistry 201 (2016) 205–212.

[18]. H. Yue, Z. Shi, Q. Wang, T. Du, Y. Ding, J. Zhang, N. Huoa and S. Yang, In situ preparation of cobalt doped ZnO@C/CNT composites by the pyrolysis of a cobalt doped MOF for high performance lithium ion batteries, RSC Adv. 5 (2015) 75653-75658.

[19]. Z. Bai, Y. Zhang, N. Fan, C. Guo, B. Tang, One-step synthesis of ZnO@C nanospheres and their enhanced performance for lithium-ion batteries, Materials Letters 119 (2014) 16–19.